AMERICAN ACADEMY OF OPHTHALMOLOGY®

Longitudinal Analysis of Retinal Microvascular and Choroidal Imaging Parameters in Parkinson's Disease Compared with Controls

Anita Kundu, BS,[1,2] Justin P. Ma, MD,[1,2] Cason B. Robbins, MD,[1,2] Praruj Pant, BS,[1,2] Vithiya Gunasan,[4] Rupesh Agrawal, MMed,[4,5] Sandra Stinnett, DrPH,[1,2] Burton L. Scott, MD, PhD,[2,3] Kathryn P.L. Moore, MD,[2,3] Sharon Fekrat, MD, FASRS,[1,2,3,*] Dilraj S. Grewal, MD, FASRS[1,2,*]

Purpose: To quantify rate of change of retinal microvascular and choroidal structural parameters in subjects with Parkinson's disease (PD) compared with controls using OCT and OCT angiography (OCTA).

Design: Prospective longitudinal study.

Participants: Seventy-four eyes of 40 participants with PD and 149 eyes of 78 control individuals from the Eye Multimodal Imaging in Neurodegenerative Disease database.

Methods: Subjects underwent OCT and OCTA imaging at 2 time points approximately 12 months apart.

Main Outcome Measures: Imaging parameters included central subfield thickness, ganglion cell-inner plexiform layer (GC-IPL) thickness, peripapillary retinal nerve fiber layer thickness, choroidal vascularity index, superficial capillary plexus perfusion density (PFD), vessel density (VD), and foveal avascular zone area.

Results: Participants with PD had greater rate of yearly decrease in GC-IPL (PD = −0.403μm, control = + 0.128 μm; $P = 0.01$), greater yearly decline in PFD in the 3 × 3 mm ETDRS circle (PD = −0.016, control = + 0.002; $P < 0.001$) and ring (PD = −0.016, control = + 0.002; $P < 0.001$); 6 × 6 mm ETDRS circle (PD = −0.021, control = 0.00; $P = 0.001$), and outer ring (PD = −0.022, control = 0.00; $P = 0.001$). Participants with PD had greater rate of yearly decline in VD in 3 × 3 mm circle (PD = −0.939/mm, control = + 0.006/mm; $P < 0.001$) and ring (PD = −0.942/mm, control = + 0.013/mm; $P < 0.001$); 6 × 6 mm circle (PD = −0.72/mm, control = −0.054/mm; $P = 0.006$), and outer ring (PD = −0.746/mm, control = −0.054/mm; $P = 0.005$). When stratified by PD severity based on Hoehn and Yahr stage, faster rates of decline were seen in Hoehn and Yahr stages 3 to 4 in the 3 × 3 mm circle PFD and VD as well as 3 × 3 mm ring VD.

Conclusions: Individuals with PD experience more rapid loss of retinal microvasculature quantified on OCTA and more rapid thinning of the GC-IPL than controls. There may be more rapid loss in patients with greater disease severity.

Financial Disclosure(s): The author(s) have no proprietary or commercial interest in any materials discussed in this article.

Parkinson's disease (PD) is a progressive neurodegenerative disorder characterized by 4 cardinal features: bradykinesia, rigidity, resting tremor, and eventual postural instability.[1] Although the underlying etiology remains unknown, PD has been associated with various neuropathologic processes, including neuronal loss in the substantia nigra and widespread α-synuclein accumulation leading to neurotoxicity.[2] Although the definitive test for diagnosis of PD is the postmortem histologic finding of α-synuclein-positive inclusions in neuronal cells, PD is currently diagnosed through clinical evaluation in conjunction with tools, such as the Unified PD Rating Scale, which assess the extent of impairment characteristics, including finger tapping, foot tapping, hand movement, facial expression, and body bradykinesia.[3] Even with these standardized scales; however, there is a variability in expert clinical diagnosis.[3,4] Biomarker correlations with PD in vivo are limited because of the invasive nature of most diagnostic approaches that assess central nervous system pathology. There remains a large unmet need for specific, noninvasive biomarkers to assist in screening, diagnosis, and monitoring of disease progression of PD.

Multimodal retinal imaging is at the forefront of a growing research effort to investigate the relationship between cerebral changes in PD and ophthalmic manifestations. OCT and OCT angiography (OCTA) are noninvasive imaging methods that present an opportunity to characterize the retina and optic nerve, a direct extension of the brain and potential surrogate for central nervous system changes.[5–7] Parkinson's disease has been associated with various molecular, cellular, and tissue-level changes in the retina, including retinal thinning and nigral dopaminergic loss.[8–10]

https://doi.org/10.1016/j.xops.2023.100393
ISSN 2666-9145/23

Prior research from our group has described retinal changes in a cross-sectional cohort of individuals with PD, including decreased retinal vessel density (VD) and decreased choroidal vascularity index (CVI).[6] Other imaging studies employing OCT have found structural evidence for foveal dysfunction and retinal dopamine loss in individuals with PD.[11] To date, other studies describing differences in the retina of individuals affected by PD have also been cross-sectional.[6,12,13]

Because PD has a disease course averaging 14.6 years, it is necessary to study changes in retinal structural and microvascular parameters over time.[14] Such data will improve our understanding of the pathophysiology of PD, contextualize findings of previous studies, and clarify whether the rate of retinal and choroidal changes in patients with PD is different from those attributed to normal aging.[15] To evaluate whether such differences exist, we compared the rate of change in retinal and choroidal imaging parameters between individuals with normal cognition and individuals with an expert-confirmed diagnosis of PD in this longitudinal study.

Methods

Protocol

This prospective longitudinal study (clinicaltrials.gov identifier NCT03233646) was approved by the Duke Health Institutional Review Board (Pro00082598) before participant enrollment. The study followed the Health Insurance Portability and Accountability Act of 1996 and adhered to all tenets of the Declaration of Helsinki. Written informed consent was provided by all study subjects or their legally authorized representative before study participation.

Participants

Case individuals were recruited from the Eye Multimodal Imaging in Neurodegenerative Disease database of patients with an expert-confirmed diagnosis of PD who had been imaged $\geq$ 12 months prior ($\pm$ 2 months). Participants with PD were identified by a movement disorders neurologist (B.L.S. and K.P.L.M.) and required clinical features of limb rigidity and bradykinesia with or without resting tremor, and responsiveness to dopaminergic therapy, in the absence of other causes of parkinsonism, such as stroke, tumor, and use of dopamine receptor-blocking drugs. Parkinson's disease stage was evaluated during an expert movement disorders neurologist (B.L.S. and K.P.L.M.) clinical examination according to Hoehn and Yahr (HY) staging.[16] The control group consisted of cognitively normal individuals without PD aged $\geq$ 50 years who had been imaged $\geq$ 12 months prior ($\pm$ 2 months). Subjects with prior retinal surgery, significant head tremor, diabetes, uncontrolled hypertension, glaucoma, history of retinal or optic nerve pathology, refractive errors $>$ + 6.0 or $-$6.0 diopters (D),[17] or corrected visual acuity $<$ 20/40 on the day of image acquisition were excluded. Ultrawidefield fundus photography was performed at both study visits and images were reviewed for retinal, choroidal, and optic nerve pathology that could confound image analysis; individuals with such pathology were excluded. All study participants had cognitive function evaluated by trained study personnel on the day of image acquisition using the Mini-Mental State Examination, an 11-question test that measures 5 areas of cognitive function for a total score of 30.[18] Control participants with a Mini-Mental State Examination score of $<$ 28 were excluded. Years of education from the first grade onward was recorded for all participants.

Image Acquisition

Nonmydriatic images were acquired by experienced Eye Multimodal Imaging in Neurodegenerative Disease study personnel using the Zeiss Cirrus High-Definition-5000 Spectral-Domain OCT with AngioPlex (version 11.0.0.29946, Carl Zeiss Meditec). Active retinal motion tracking was used to reduce motion artifact during acquisition. Follow-up OCT and OCTA images were registered to study entry visits using the inbuilt retinal tracking function, allowing for precise point-to-point measurements of change in each patient. Only patients with registered images were included in the study. All images were individually reviewed manually by trained study personnel for quality assessment. Those that had $<$ 7 of 10 signal strength index, segmentation artifact, motion artifact, shadow artifact, or focal signal loss that would impact the assessment of the quantitative variables were then separately reviewed by a second expert image grader (D.S.G.) for concurrence of poor image quality and excluded from the study to avoid confounding of imaging results because of poor image quality.

OCT Image Acquisition

One 200 $\times$ 200 optic disc cube, 1 high definition 21-line with enhanced depth imaging foveal scan, and one 512 $\times$ 128 macular cube scan was acquired for each eye. Average retinal nerve fiber layer (RNFL) thickness in µm was automatically quantified from the 200 $\times$ 200 optic disc cube within a 3.46-mm diameter circle centered on the optic disc. Ganglion cell-inner plexiform layer (GC-IPL) thickness was automatically quantified by the Cirrus software from the macula cube scans, derived from a 14.13 mm^2 elliptical annulus centered on the fovea with an inner vertical radius of 0.5 mm and outer vertical radius of 2 mm. The thickness parameters derived from the macula scan were the average GC layer plus IPL thickness across the entire elliptical annulus as well as the thickness at six 60° sectors of the elliptical annulus (Fig 1). Central subfield thickness (CST) was measured using the macular cube 512 $\times$ 128 scan, defined as the thickness of the retina in the central 1-mm ETDRS subfield measured between the internal limiting membrane and the inner third of the retinal pigment epithelium.

Choroidal vascularity index was measured using the high definition 21-line enhanced depth imaging foveal scan. The deidentified scans were uploaded to Comprehensive Ocular Imaging Network online portal (www.ocularimaging.net) and analyzed using the built-in algorithm.[19] The choroid, defined as the area between the outer border of the hyperreflective retinal pigment epithelium and the sclerochoroidal junction, was measured using the Comprehensive Ocular Imaging Network software within a 1500 µm wide region of interest centered on the fovea. Once outlined by the software, the region of interest was manually reviewed by a trained image grader (A.K.) and further reviewed for accuracy by a retina specialist grader (R.A.). Images that had artifact that would impact grading based on the graders' judgment or were of low resolution based on obscuration of the subfoveal choroid were excluded from analysis. OCT images underwent automated binarization using the Comprehensive Ocular Imaging Network software. Total choroidal area (TCA) was defined as the total area in pixels within the region of interest, and luminal area (LA) was measured as the area of binarized dark pixels in the choroid, representing the vascular lumen area. Choroidal vascularity index was then calculated by dividing LA by TCA, representing the ratio of vascular lumen area to TCA (Fig 2).

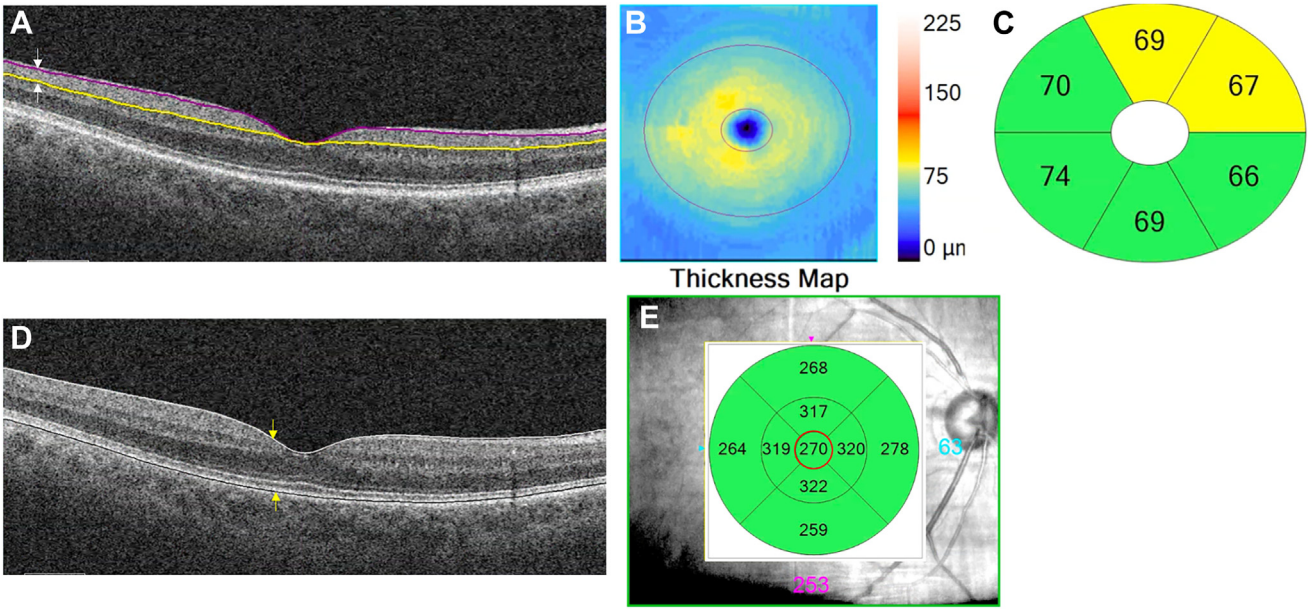

Figure 1. Ganglion cell inner plexiform layer (GC-IPL) thickness and central subfield measurements. **A**, The outer border of the retinal nerve fiber layer (RNFL) is represented by the solid purple line and the outer border of IPL is represented by the solid yellow line. The difference between the RNFL and the IPL outer boundary segmentations yields the combined thickness of the ganglion cell layer and the IPL. **B**, GC-IPL thickness maps (the denser the yellow ring, the thicker the GC-IPL) calculated in an elliptical annulus (dimensions: vertical inner and outer radius of 0.5 mm and 2.0 mm, horizontal inner and outer radius [purple lines] of 0.6 and 2.4 mm, respectively) (area between the two purple rings) within the cube used by the Cirrus GCA algorithm to measure the thickness of the GC-IPL. **C**, The average and sectoral (superotemporal, superior, superonasal, inferonasal, inferior, and inferotemporal) thicknesses of the GC-IPL are measured in this elliptical annulus. **D**, Central subfield thickness (CST) measurement. The Cirrus segmentation software algorithm defines retinal thickness as the distance between the ILM (top yellow arrow) to the inner one-third of the retinal pigment epithelium (bottom yellow arrow). **E**, Retinal thickness map displayed for each subfield of the ETDRS grid. CST (red circle) was defined as the average thickness of the retina in the central 1 mm ETDRS grid.

OCTA Image Acquisition

For each eye, 3 × 3 mm and 6 × 6 mm scans centered on the fovea were acquired. Foveal avascular zone area (mm^2) was calculated using the 3 × 3 mm superficial capillary plexus image. The inner boundary of the superficial capillary plexus was the internal limiting membrane, and the outer boundary was the IPL. In cases of machine segmentation error or inaccurate boundaries, a trained grader manually reviewed and adjusted boundaries, and this was confirmed by an experienced retina specialist (D.S.G.). Both VD and perfusion density (PFD) were automatically quantified by integrated Cirrus software, allowing the algorithmic analysis of retinal microvasculature in the 9 subfields corresponding to the ETDRS using 3 × 3 mm and 6 × 6 mm scans centered on the fovea (Fig 3).[20] Vessel density was defined as the total length of perfused vasculature per unit area within the region of measurement (measured as mm/mm^2). Plexus perfusion density was defined as the total area of perfused vasculature per unit area in the region of measurement (measured as percentage). For the 3 × 3 mm scans, VD and PFD were measured in the EDTRS 3-mm circle and 3-mm ring. For 6 × 6 mm scans, the VD and PFD were measured in the ETDRS 6-mm circle, 6-mm inner ring, and 6-mm outer ring.

Statistical Analysis

Data analysis was generated using SAS/STAT software (version 9.4 of the SAS System for Windows 2002–2012, SAS Institute Inc) by an experienced statistician (S.S.S.). Demographic variables were compared overall across groups. *P* values for continuous variables were calculated using Wilcoxon rank sum test. *P* values for categorical variables were calculated using Fisher exact test. To calculate the rate of change in imaging parameters, the value at the study entry visit was subtracted from the value at the follow-up visit. This number was divided by the time in years between visits. Rate of change was then used as a comparison point between groups. Multivariate generalized estimating equations were used to compare OCT and OCTA parameters between groups to account for inclusion of 2 eyes from the same individual, and models were adjusted for age and sex. Statistical significance was defined by a *P* value of < 0.05.

Results

Seventy-four eyes of 40 subjects with PD and 149 eyes of 78 control subjects were included in this study. Nine eyes of PD participants and 8 eyes of controls were excluded from analysis because of poor scan quality. Four eyes of PD participants were excluded for poor visual acuity. One control eye was excluded due to retinal pathology. Demographic composition of the groups is shown in Table 1. There was a higher proportion of men in the PD group (PD = 60%, control = 28% male; $P = 0.001$). Although there was a significant difference in Mini-Mental State Examination score between the groups (PD = 29 ± 1.4, control = 29.5 ± 0.8; $P = 0.019$), both groups had a mean score of > 27.

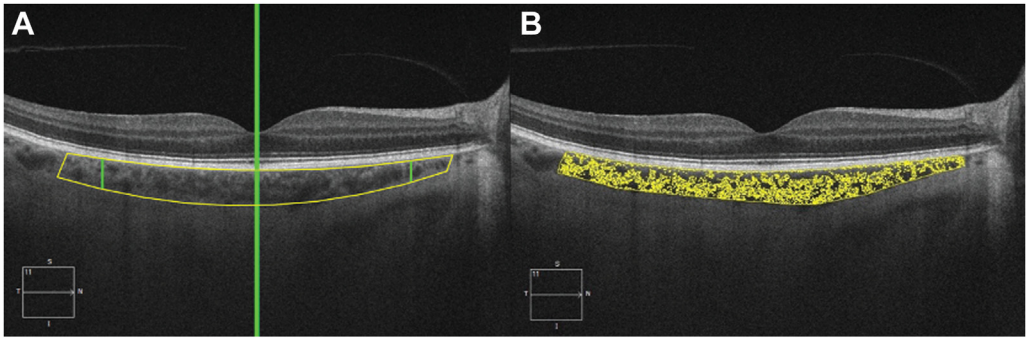

Figure 2. A region of interest in the enhanced depth imaging foveal scan was demarcated using the yellow markers (**A**), representing the total choroidal area (TCA) within a standard span of 1500 μm (green markers). The image was binarized (**B**) using Comprehensive Ocular Imaging Network software and choroidal vascularity index was calculated by dividing luminal area by TCA.

Study entry OCT and OCTA parameters are shown in Table 2. Participants with PD and controls did not differ significantly in CST, GC-IPL thickness, or RNFL thickness. There was a significant difference in the following OCT imaging parameters: TCA ($P < 0.001$), LA ($P < 0.001$), and CVI ($P < 0.001$). Between the 2 groups, there was a significant difference at study entry in the following OCTA imaging parameters, being lower in the participants with PD: 6 × 6 mm circle PFD ($P = 0.012$), 6 × 6 mm inner ring PFD ($P = 0.012$), 6 × 6 mm outer ring ($P = 0.021$), 6 × 6 mm circle VD ($P = 0.007$), 6 × 6 mm inner ring VD ($P = 0.001$), and 6 × 6 outer ring VD ($P = 0.018$).

After a mean interval of 22.8 months (range, 10.2−43.2 months), participants with PD and controls were reimaged. Table 3 illustrates the association between PD status and rate of change in retinal and choroidal imaging parameters**.** There was a significant difference in GC-IPL thickness rate of change ($P = 0.01$). There were significantly faster rates of yearly decline in participants with PD compared with controls in the following OCTA parameters: 3 × 3 mm circle PFD ($P < 0.001$), 3 × 3 mm ring PFD ($P < 0.001$), 6 × 6 mm circle PFD ($P = 0.001$), 6 × 6 mm inner ring PFD ($P = 0.007$), 6 × 6 mm outer ring PFD ($P = 0.001$), 3 × 3 mm circle VD ($P < 0.001$), 3 × 3 mm ring VD ($P < 0.001$), 6 × 6 mm circle VD ($P = 0.006$), 6 × 6 mm inner ring VD ($P = 0.03$), and 6 × 6 mm outer ring VD ($P = 0.005$). There was no significant difference in rate of change between PD participants and controls in foveal avascular zone area, CST, RNFL thickness, TCA, LA, or CVI.

To analyze the differences in rate of change stratified by HY stage, HY stages were clustered into 3 groupings by expert neurologists (B.L.S. and K.P.M.): HY stage 1−1.5, HY stage 2−2.5, and HY stage 3−4. The analysis revealed a significant difference in rate of change with faster rates of decline seen in HY stage 3−4 (Table 4) in the 3 × 3 mm circle PFD and VD as well as 3 × 3 mm ring VD.

Thirty-nine of 40 patients with PD in our study were taking levodopa at study entry and continued it during the study period. As almost all the participants were on levodopa in this cohort, we could not evaluate for levodopa-associated differences.

Discussion

There has been increasing effort to identify ophthalmic biomarkers to assist in both PD screening and diagnosis as well as PD progression for which longitudinal data of imaging parameters are required. In neurogenerative diseases, ocular biomarkers have in general a moderate diagnostic accuracy in cross-sectional studies and longitudinal studies and are critical to detect earlier changes as well as the rate of change. In PD, longitudinal data quantifying the rate of change of retinal and choroidal metrics and their difference from normal aging are lacking. In this longitudinal study of 74 PD eyes and 149 control eyes, we observed higher rates of yearly loss, often multiple times higher, in VD, PFD, and GC-IPL thickness in patients with PD than in controls over a mean interval of 22.8 months. Although the imaging interval between cohorts was not identical, this was accounted for by calculating the change in imaging parameter over time rather than a raw measurement. The findings of this study suggest that individuals with PD may experience more rapid loss of microvasculature and faster rates of neurodegenerative decline in the retina than controls. In addition, the velocity of decline may be greater in those with more severe PD as quantified by the HY stage; however, additional work with a larger sample size would be needed to confirm this observation.

There is no consensus on the relationship between CST, GC-IPL, and RNFL thickness and PD on cross-sectional studies as different OCT imaging platforms have yielded different results. [6,21−23] Our finding of no significant difference in RNFL thickness both cross-sectionally and longitudinally suggests that further studies with larger cohorts and a longer timeframe may be needed to elucidate the relationship between PD and RNFL thickness.[6,22] Although we did not find a significant cross-sectional difference in GC-IPL thickness between PD and control patients, participants with PD had a significantly greater rate of GC-IPL thinning over time. This is an important finding because 2 years is a relatively short span in the continuum of PD, and the differences may be exaggerated over a longer follow-up. The data suggest that there may be possible utility of

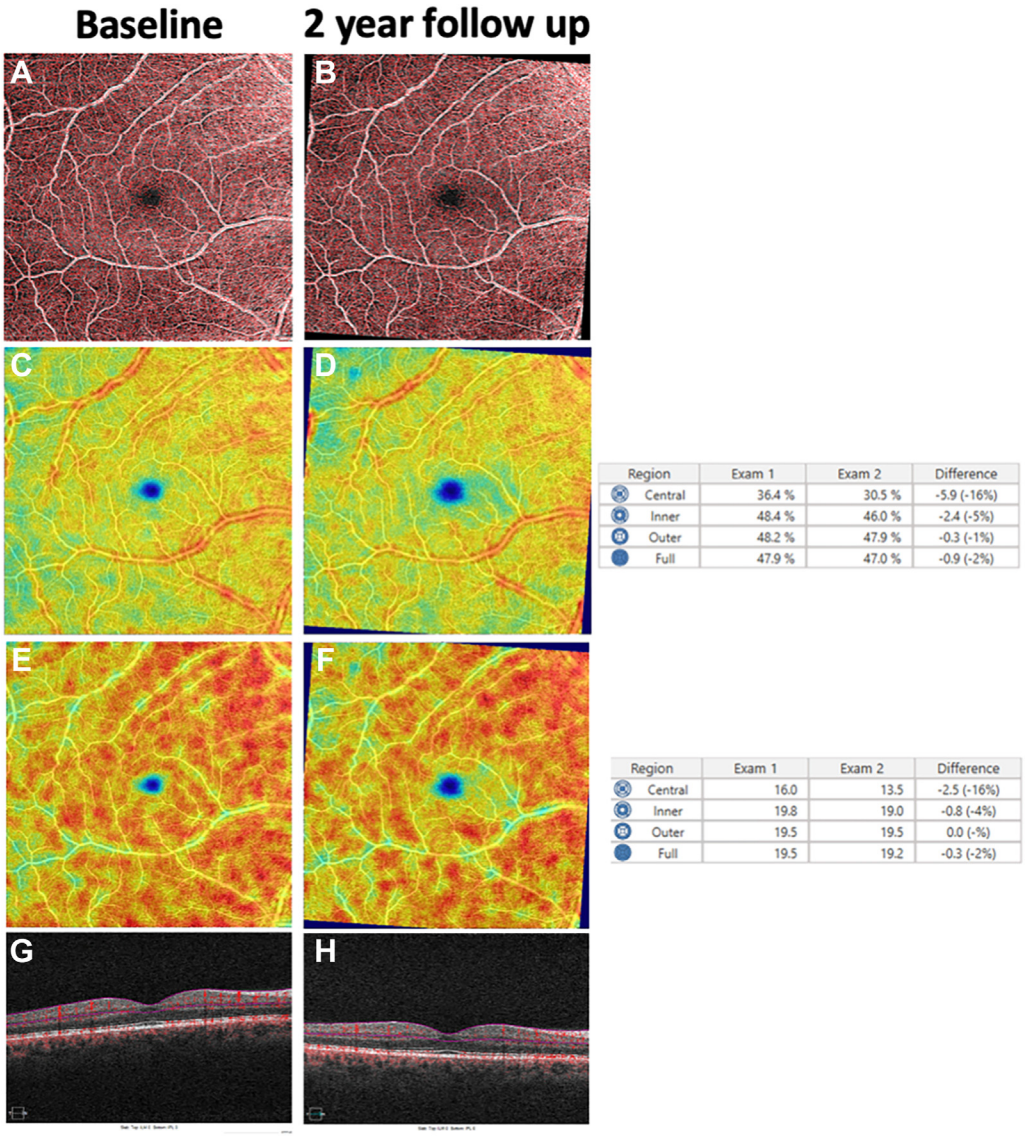

Figure 3. A 62-year-old man with Parkinson's disease (Hoehn-Yahr Stage 4) with a Mini-Mental State Examination score of 29 at baseline visit in December 2017. OCT angiography image (6 × 6 mm) of the superficial capillary plexus with binarization for vessel density measurements at study entry baseline (**A**) and the registered follow-up image at the 2-year follow-up in January 2020 (**B**). Color coded maps showing perfusion density (**C**) at baseline and follow-up (**D**) showing reduction in perfusion density in the inner (3 mm) and outer (6 mm) ETDRS grids. Color coded maps showing vessel density (**E**) at baseline and follow-up (**F**) showing reduction in vessel density in the inner (3 mm) and 6 mm ETDRS grids. Structural OCT image with flow overlay at baseline (**G**) and registered image at follow-up (**H**) showing segmentation lines of the superficial capillary plexus—internal limiting membrane and inner plexiform layers.

monitoring GC-IPL thickness as a surrogate for progression of dopaminergic neurodegeneration.[24]

Total choroidal area, LA, and CVI were significantly different between PD and controls at each cross-sectional time point, similar to our prior findings, and may be related to the vasodilatory effects of D1 dopamine receptors.[6] There was, however, no significant difference in the rates of change of these choroidal parameters between PD and control groups during the 2 years studied. Longer follow-up periods may help to determine if there are differences in the rates of change of CVI in PD or the differences are limited to retinal parameters. Previous longitudinal studies in controls have not found significant CVI changes over time periods spanning < 5 years, which may also suggest that choroidal changes may take longer to manifest.[25]

To our knowledge, there are no longitudinal studies exploring the association of PFD and VD in patients with PD. Our longitudinal data exhibited significantly higher rates of VD and PFD loss in patients with PD than in controls. Vascular degeneration and capillary fragmentation have been well described in PD, particularly in the substantia nigra, and it may be speculated that such changes also occur in the retina and present as neurodegeneration

Table 1. Demographic Characteristics of Study Participants

Variable	Parkinson's (n = 40)	Control (n = 78)	*P* Value*
Age in yrs, mean (SD)	67.4 (7.9)	70.3 (5.8)	0.065
Male, N (%)	24 (60)	22 (28)	0.001
Race, N (%)			0.265
White	38 (95)	77 (99)	
Black/African American	0	1 (1)	
American Indian/Alaskan Native	1 (2.5)	0	
Other	1 (2.5)	0	
Family history, N (%)	18 (45)	45 (58)	0.243
HY stage time 1, N (%)			
1	4 (10)		
1.5	3 (7.5)		
2	20 (50)		
2.5	8 (20)		
3	4 (10)		
4	1 (2.5)		
HY stage time 2, N (%)			
1	3 (7.5)		
1.5	3 (7.5)		
2	19 (47.5)		
2.5	10 (25)		
3	3 (7.5)		
4	2 (5)		
MMSE, mean (SD)	29 (1.4)	29.5 (0.8)	0.019

HY = Hoehn and Yahr; MMSE = Mini-Mental State Examination; N = number; SD = standard deviation.
**P* value for continuous variables based on Wilcoxon rank sum test. *P* value for categorical variables based on Fisher exact test.

Table 2. Retinal and Choroidal Imaging Parameters at Study Entry

Parameters	Parkinson's N = 74 Eyes (40 Subjects) Mean (SD)	Control N = 149 Eyes (78 Subjects) Mean (SD)	*P* Value*
OCT parameters			
CST, μm	270.4 (23.03)	268.4 (21.13)	0.787
Mean GC-IPL thickness, μm	76.14 (7.882)	76.29 (6.780)	0.494
Mean RNFL thickness, μm	88.11 (9.355)	88.15 (8.911)	0.476
TCA	7739.0 (1904.4)	5956.8 (1673.2)	< 0.001
LA	4981.0 (1193.4)	3982.5 (1102.4)	< 0.001
CVI, %	64.502 (1.971)	67.490 (3.045)	< 0.001
OCTA parameters			
FAZ area, mm^2	0.209 (0.101)	0.235 (0.094)	0.247
PFD (3 × 3 mm circle)	0.361 (0.035)	0.358 (0.040)	0.704
PFD (3 × 3 mm ring)	0.381 (0.036)	0.378 (0.041)	0.643
PFD (6 × 6 mm circle)	0.431 (0.038)	0.436 (0.047)	0.012
PFD (6 × 6 mm inner ring)	0.422 (0.043)	0.430 (0.048)	0.012
PFD (6 × 6 mm outer ring)	0.441 (0.038)	0.445 (0.048)	0.021
VD (3 × 3 mm circle)	20.09 (2.124)	20.14 (1.615)	0.250
VD (3 × 3 mm ring)	21.11 (2.211)	21.17 (1.614)	0.208
VD (6 × 6 mm circle)	17.62 (1.494)	17.95 (1.037)	0.007
VD (6 × 6 mm inner ring)	17.56 (1.678)	18.13 (1.185)	0.001
VD (6 × 6 mm outer ring)	17.92 (1.511)	18.16 (1.075)	0.018

CST = central subfield thickness; CVI = choroidal vascularity index; FAZ = foveal avascular zone; GC-IPL = ganglion cell-inner plexiform layer; LA = luminal area; OCTA = OCT angiography; PFD = perfusion density; RNFL = retinal nerve fiber layer; SD = standard deviation; TCA = total choroidal area; VD = vessel density.
**P* value based on test of difference between choroidal groups were adjusted for age and sex and used generalized estimating equations to control for correlation between eyes.

Table 3. Rate of Change of Retinal and Choroidal Imaging Parameters

Parameters	Parkinson's N = 74 Eyes (40 Subjects) Mean (SD)	Control N = 149 Eyes (78 Subjects) Mean (SD)	*P* Value*
Follow-up time in yrs	1.489 (0.620)	2.101 (0.279)	< 0.001
OCT parameters			
CST, μm	0.580 (16.120)	−0.657 (2.585)	0.913
Mean GC-IPL thickness, μm	−0.403 (1.010)	0.128 (1.219)	0.010
Mean RNFL thickness, μm	−0.090 (3.063)	0.249 (1.815)	0.807
TCA	208.88 (830.07)	−55.97 (540.77)	0.158
LA	97.664 (492.82)	−31.46 (340.81)	0.297
CVI, %	−0.620 (2.039)	−0.009 (1.316)	0.051
OCTA parameters			
FAZ area, mm^2	−0.001 (0.037)	0.002 (0.016)	0.377
PFD (3 × 3 mm circle)	−0.016 (0.027)	0.002 (0.015)	< 0.001
PFD (3 × 3 mm ring)	−0.016 (0.028)	0.002 (0.015)	< 0.001
PFD (6 × 6 mm circle)	−0.021 (0.039)	0.000 (0.015)	0.001
PFD (6 × 6 mm inner ring)	−0.018 (0.041)	0.001 (0.018)	0.007
PFD (6 × 6 mm outer ring)	−0.022 (0.040)	0.000 (0.016)	0.001
VD (3 × 3 mm circle)	−0.939 (1.489)	0.006 (0.876)	< 0.001
VD (3 × 3 mm ring)	−0.942 (1.565)	0.013 (0.903)	< 0.001
VD (6 × 6 mm circle)	−0.720 (1.469)	−0.054 (0.599)	0.006
VD (6 × 6 mm inner ring)	−0.636 (1.595)	−0.048 (0.704)	0.030
VD (6 × 6 mm outer ring)	−0.746 (1.513)	−0.054 (0.625)	0.005

CST = central subfield thickness; CVI = choroidal vascularity index; FAZ = foveal avascular zone; GC-IPL = ganglion cell-inner plexiform layer; LA = luminal area; OCTA = OCT angiography; PFD = perfusion density; RNFL = retinal nerve fiber layer; SD = standard deviation; TCA = total choroidal area; VD = vessel density.
**P* value based on test of difference between choroidal groups were adjusted for age and sex and used generalized estimating equations to control for correlation between eyes.

Table 4. Rate of Change of Retinal and Choroidal Imaging Parameters Stratified by PD Severity

Parameters	HY Stage 1−1.5 (n = 9) Mean (SD)	HY Stage 2−2.5 (n = 47) Mean (SD)	HY Stage 3−4 (n = 8) Mean (SD)	*P* Value*
OCT parameters				
CST, μm	−0.419 (2.354)	1.713 (18.473)	−4.843 (10.337)	0.271
Mean GC-IPL thickness, μm	−0.381 (0.416)	−0.422 (1.152)	−0.426 (0.683)	0.982
Mean RNFL thickness, μm	0.885 (1.443)	−0.139 (3.305)	−1.215 (2.981)	0.066
TCA	−124.8 (524.04)	284.58 (829.00)	164.74 (1279.9)	0.654
LA	−143.4 (309.59)	153.42 (505.49)	55.806 (604.63)	0.609
CVI, %	−0.826 (1.491)	−0.546 (2.040)	−0.903 (3.203)	0.781
OCTA parameters				
FAZ area, mm^2	−0.026 (0.046)	0.003 (0.037)	0.001 (0.020)	0.235
PFD (3 × 3 mm circle)	−0.025 (0.040)	−0.012 (0.022)	−0.033 (0.026)	0.047
PFD (3 × 3 mm ring)	−0.026 (0.043)	−0.012 (0.023)	−0.034 (0.028)	0.062
PFD (6 × 6 mm circle)	−0.033 (0.042)	−0.019 (0.037)	−0.025 (0.050)	0.437
PFD (6 × 6 mm inner ring)	−0.016 (0.052)	−0.016 (0.040)	−0.029 (0.043)	0.641
PFD (6 × 6 mm outer ring)	−0.039 (0.040)	−0.020 (0.039)	−0.023 (0.052)	0.293
VD (3 × 3 mm circle)	−1.422 (2.201)	−0.646 (1.236)	−2.121 (1.353)	0.009
VD (3 × 3 mm ring)	−1.498 (2.313)	−0.626 (1.298)	−2.171 (1.418)	0.018
VD (6 × 6 mm circle)	−1.134 (1.604)	−0.650 (1.423)	−0.731 (1.823)	0.489
VD (6 × 6 mm inner ring)	−0.529 (2.014)	−0.605 (1.547)	−0.977 (1.676)	0.732
VD (6 × 6 mm outer ring)	−1.348 (1.485)	−0.662 (1.473)	−0.638 (1.919)	0.273

CST = central subfield thickness; CVI = choroidal vascularity index; FAZ = foveal avascular zone; GC-IPL = ganglion cell-inner plexiform layer; HY = Hoehn and Yahr; LA = luminal area; OCTA = OCT angiography; PD = Parkinson's disease; PFD = perfusion density; RNFL = retinal nerve fiber layer; SD = standard deviation; TCA = total choroidal area; VD = vessel density.
**P* value based on test of difference between choroidal groups were adjusted for age and sex and used generalized estimating equations to control for correlation between eyes.

detected by GC-IPL thinning and loss of microvasculature detected by PFD and VD decrease.[26,27] There may also be a cumulative effect of the progression of α-synuclein deposition and microvascular regression that occurs in PD throughout the disease course, contributing to the faster velocity of these changes in PD eyes than in controls and a disease severity-dependent effect.[28]

Our study was comprised of patients with PD mostly in earlier stages of PD, with a median HY score of 2 at study entry. When results were stratified by HY stage, there was a significant difference in 3 × 3 mm circle PFD and VD as well as the 3 × 3 mm ring VD, suggesting faster rates of decline in more advanced stages of PD. These results should be considered in the context that the distribution of individuals across HY stages was not equally distributed, with 47 eyes in the HY 2 and 2.5 category and only 8 eyes in the HY 3 and 4 category. Individuals with more advanced PD often have tremor and involuntary motion that precludes capture of images of interpretable quality, which may not always be compensated for by the built-in motion correction system; however, the clinical diagnosis of PD is more definitive in these later stages, negating the proposed benefits of retinal and choroidal imaging in the earlier diagnosis of PD. When advances in retinal imaging device software do allow for better eye tracking and motion reduction; however, future studies may include a larger number of subjects at more advanced PD stages and motor symptoms to further assess the extent of retinal and choroidal changes that may occur in severe PD.

Axial length was not routinely measured via A-scan in study participants; however, we excluded individuals with a spherical equivalent of $\geq$ 6 D in magnitude to minimize any potential effect of axial length on OCTA measurements.[17] Sampson et al[17] found that eyes with spherical equivalents between −8 D and + 5 D were predicted to correspond to < 5% change in macular OCTA parameters. This study also suggested that as the parafoveal region had a relatively uniform vascular network in healthy eyes, small changes in its boundary from image size correction due to differences in axial length were less likely to induce significant change in overall density.[17]

Parkinson's disease is 1.5 times more common in men than in women, which likely played a role in the higher ratio of male sex among participants with PD than controls in this study.[29] This was accounted for in the statistical analysis by controlling for sex. Although many studies have explored sex differences in retinal microvasculature, there is no consensus thus far on the relationship between sex and retinal imaging parameters, such as foveal avascular zone and macular VD, in neurodegenerative diagnoses.[30,31] Additionally, there are no sufficient longitudinal studies to draw conclusions on differences in rate of change of imaging parameters between men and women. Levodopa has been shown to dilate choroidal vessels.[32] As almost all the participants were on levodopa in this cohort (39 of 40), we could not evaluate for potential differences in rates of change related to levodopa use. Although we aimed to try to evaluate the relationship between levodopa use and CVI in further investigations, it may be challenging as dopaminergic replacement is typically prescribed early in the disease in those with symptomatic PD under the care of neurologists.

This study is among the first to explore longitudinal changes in retinal and choroidal imaging parameters between individuals with PD and controls.[6,33] Notably, we found that over 2 years, there is a significantly greater velocity of decrease in PFD, VD, and GC-IPL thickness in participants with PD than in controls, suggesting that patients with PD may experience more rapid loss of retinal microvascular perfusion and VD as well as more rapid thinning of the GC-IPL compared with cognitively normal controls without PD, in just 2 years. With the longitudinal study design, we compared imaging parameters within the same eye, which helps better contextualize findings. The robust inclusion and exclusion criteria with strict image quality control helped to minimize confounding variables, and professional diagnoses of expert neurologists allowed standardization of PD diagnosis and characterization of their respective HY stages. Incorporation of retinal and choroidal parameters as a supporting target in clinical trials investigating disease-modifying approaches in PD, although promising, requires further validation of these biomarkers.[34] Additional investigation will determine whether the rate of change slopes of these parameters play a role in biological stratification of disease progression.

Footnotes and Disclosures

Originally received: February 26, 2023.
Final revision: August 15, 2023.
Accepted: August 29, 2023.
Available online: September 9, 2023. Manuscript no. XOPS-D-23-00046R2.

[1] Department of Ophthalmology, Duke University School of Medicine, Durham, North Carolina.

[2] iMIND Research Group, Durham, North Carolina.

[3] Department of Neurology, Duke University School of Medicine, Durham, North Carolina.

[4] National Healthcare Group Eye Institute, Tan Tock Seng Hospital, Singapore.

[5] Lee Kong Chian School of Medicine, Nanyang Technological University, Singapore.

*S.F. and D.S.G. contributed equally to this work.

Presented at the 2022 Association for Research in Vision and Ophthalmology (ARVO) meeting (May 2022; Denver, Colorado), 2022 Duke Eye Center Residents and Fellows Day (June 2022; Durham, North Carolina), 2022 XXXIII Meeting of the Club Jules Gonin (September 2022; Dubrovnik, Croatia), American Society of Retina Specialists (ASRS) 2022 Meeting (July 2022; New York City, New York), 2022 Alzheimer's Association International Conference (AAIC) (July 2022; San Diego, CA), 2022 Women in Ophthalmology (WIO) Symposium (August 2022; Monterey, CA), and 2022 North Carolina Society of Eye Physicians and Surgeons (NCSEPS) Annual Meeting (September 2022; Greensboro, NC).

Disclosures:

All authors have completed and submitted the ICMJE disclosures form.

The authors made the following disclosures:

Supported by the Research to Prevent Blindness Unrestricted Grant (A.K.).

HUMAN SUBJECTS: Human subjects were included in this study. This longitudinal study (clinicaltrials.gov identifier NCT03233646) was approved by the Duke Health Institutional Review Board (Pro00082598) before participant enrollment. The study followed the Health Insurance Portability and Accountability Act of 1996 and adhered to all tenets of the Declaration of Helsinki. Written informed consent was provided by all study subjects or their legally authorized representative before study participation.

No animal subjects were used in this study.

Author Contributions:

Conception and design: Kundu, Scott, Moore, Fekrat, Grewal

Data collection: Kundu, Ma, Robbins, Pant, Scott, Moore, Fekrat, Grewal

Analysis and interpretation: Kundu, Robbins, Pant, Gunasan, Agarwal, Stinnett, Fekrat, Grewal

Obtained funding: Kundu

Overall responsibility: Kundu, Fekrat, Grewal

Abbreviations and Acronyms:
CST = central subfield thickness; **CVI** = choroidal vascularity index; **D** = diopters; **GC-IPL** = ganglion cell-inner plexiform layer; **HY** = Hoehn and Yahr; **IPL** = inner plexiform layer; **LA** = luminal area; **OCTA** = OCT angiography; **PD** = Parkinson's disease; **PFD** = plexus perfusion density; **RNFL** = retinal nerve fiber layer; **TCA** = total choroidal area; **VD** = vessel density.

Keywords:
Biomarker, Neurodegeneration, OCTA, Parkinson's disease, Retina.

Correspondence:
Dilraj S. Grewal, MD, FASRS, Box 3802, DUMC, Durham, NC 27710. E-mail: iMIND@duke.edu.

References

1. Jankovic J. Parkinson's disease. clinical features and diagnosis. *J Neurol Neurosurg Psychiatry*. 2008;79(4):368−376.
2. Isaias IU, Marzegan A, Pezzoli G, et al. A role for locus coeruleus in Parkinson tremor. *Front Hum Neurosci*. 2011;5:179.
3. Ramaker C, Marinus J, Stiggelbout AM, van Hilten BJ. Systematic evaluation of rating scales for impairment and disability in Parkinson's disease. *Mov Disord*. 2002;17(5):867−876.
4. Rizzo G, Copetti M, Arcuti S, Martino D, Fontana A, Logroscino G. Accuracy of clinical diagnosis of Parkinson disease. A systematic review and meta-analysis. *Neurology*. 2016;86(6):566−576.
5. London A, Benhar I, Schwartz M. The retina as a window to the brain-from eye research to CNS disorders. *Nat Rev Neurol*. 2013;9(1):44−53.
6. Robbins CB, Thompson AC, Bhullar PK, et al. Characterization of retinal microvascular and choroidal structural changes in Parkinson disease. *JAMA Ophthalmol*. 2021;139(2):182−188.
7. Yoon SP, Thompson AC, Polascik BW, et al. Correlation of OCTA and volumetric MRI in mild cognitive impairment and Alzheimer's disease. *Ophthalmic Surg Lasers Imaging Retina*. 2019;50(11):709−718.
8. Lin JB, Apte RS. Seeing Parkinson disease in the retina. *JAMA Ophthalmol*. 2021;139(2):189−190.
9. Hajee ME, March WF, Lazzaro DR, et al. Inner retinal layer thinning in Parkinson disease. *Arch Ophthalmol*. 2009;127(6):737−741.
10. Ahn J, Lee JY, Kim TW, et al. Retinal thinning associates with nigral dopaminergic loss in de novo Parkinson disease. *Neurology*. 2018;91(11):e1003−e1012.
11. Lee JY, Ahn J, Kim TW, Jeon BS. Optical coherence tomography in Parkinson's disease: is the retina a biomarker? *J Parkinson's Dis*. 2014;4(2):197−204.
12. Garcia-Martin E, Rodriguez-Mena D, Satue M, et al. Electrophysiology and optical coherence tomography to evaluate Parkinson disease severity. *Invest Ophthalmol Vis Sci*. 2014;55(2):696−705.
13. Zou J, Liu K, Li F, et al. Combination of optical coherence tomography (OCT) and OCT angiography increases diagnostic efficacy of Parkinson's disease. *Quant Imaging Med Surg*. 2020;10(10):1930−1939.
14. Poewe W, Seppi K, Tanner CM, et al. Parkinson disease. *Nat Rev Dis Primers*. 2017;3:17013.
15. Golbe LI, Leyton CE. Life expectancy in Parkinson disease. *Neurology*. 2018;91(22):991−992.
16. Hoehn MM, Yahr MD. Parkinsonism: onset, progression, and mortality. 1967. *Neurology*. 2001;57(10 Suppl 3):S11−S26.
17. Sampson DM, Gong P, An D, et al. Axial length variation impacts on superficial retinal vessel density and foveal avascular zone area measurements using optical coherence tomography angiography. *Invest Ophthalmol Vis Sci*. 2017;58(7):3065−3072.
18. Folstein MF, Folstein SE, McHugh PR. "Mini-mental state". A practical method for grading the cognitive state of patients for the clinician. *J Psychiatr Res*. 1975;12(3):189−198.
19. Agrawal R, Salman M, Tan KA, et al. Choroidal Vascularity Index (CVI)–a novel optical coherence tomography parameter for monitoring patients with panuveitis? *PLoS One*. 2016;11(1):e0146344.
20. Early Treatment Diabetic Retinopathy Study Research Group. Grading diabetic retinopathy from stereoscopic color fundus photographs — an extension of the modified airlie house classification: ETDRS report number 10. *Ophthalmology*. 2020;127(4S):S99−S119.
21. Yu JG, Feng YF, Xiang Y, et al. Retinal nerve fiber layer thickness changes in Parkinson disease: a meta-analysis. *PLoS One*. 2014;9(1):e85718.
22. Satue M, Obis J, Alarcia R, et al. Retinal and choroidal changes in patients with Parkinson's disease detected by swept-source optical coherence tomography. *Curr Eye Res*. 2018;43(1):109−115.
23. Altay L, Jahn C, Arikan Yorgun M, et al. Alteration of retinal layers in healthy subjects over 60 years of age until nonagenarians. *Clin Ophthalmol*. 2017;11:1499−1503.
24. Živković M, Dayanir V, Stamenović J, et al. Retinal ganglion cell/inner plexiform layer thickness in patients with Parkinson's disease. *Folia Neuropathol*. 2017;55(2):168−173.
25. Ma JP, Robbins CB, Lee JM, et al. Longitudinal analysis of the retina and choroid in cognitively normal individuals at higher genetic risk of Alzheimer disease. *Ophthalmol Retina*. 2022;6(7):607−619.

26. Guan J, Pavlovic D, Dalkie N, et al. Vascular degeneration in Parkinson's disease. *Brain Pathol*. 2013;23(2):154–164.
27. Kromer R, Buhmann C, Hidding U, et al. Evaluation of retinal vessel morphology in patients with Parkinson's disease using optical coherence tomography. *PLoS One*. 2016;11(8): e0161136.
28. Price DL, Rockenstein E, Mante M, et al. Longitudinal live imaging of retinal alpha-synuclein::GFP deposits in a transgenic mouse model of Parkinson's disease/dementia with Lewy bodies. *Sci Rep*. 2016;6:29523.
29. Haaxma CA, Bloem BR, Borm GF, et al. Gender differences in Parkinson's disease. *J Neurol Neurosurg Psychiatry*. 2007;78(8):819–824.
30. Shahlaee A, Samara WA, Hsu J, et al. In vivo assessment of macular vascular density in healthy human eyes using optical coherence tomography angiography. *Am J Ophthalmol*. 2016;165:39–46.
31. Mirzania D, Thompson AC, Robbins CB, et al. Retinal and choroidal changes in men compared with women with Alzheimer's disease: a case-control study. *Ophthalmol Sci*. 2022;2(1):100098.
32. Reitsamer HA, Zawinka C, Branka M. Dopaminergic vasodilation in the choroidal circulation by d1/d5 receptor activation. *Invest Ophthalmol Vis Sci*. 2004;45(3):900–905.
33. Kwapong WR, Ye H, Peng C, et al. Retinal microvascular impairment in the early stages of Parkinson's disease. *Investig Ophthalmol Vis Sci*. 2018;59(10):4115–4122.
34. Vijiaratnam N, Simuni T, Bandmann O, Morris HR, Foltynie T. Progress towards therapies for disease modification in Parkinson's disease. *Lancet Neurol*. 2021;20(7):559–572.